Journal of Geophysical Research Atmospheres

Supporting Information for

Impacts of recent warming and the 2015/16 El Niño on tropical Peruvian ice fields

L. G. Thompson[1,2], M. E. Davis[1], E. Mosley-Thompson[1,3], E. Beaudon[1], S. E. Porter[1], S. Kutuzov[4], P-N. Lin[1], V. N. Mikhalenko[4], K. R. Mountain[5]

[1]Byrd Polar and Climate Research Center, The Ohio State University, Columbus, OH 43210 USA.
[2]School of Earth Sciences, The Ohio State University, Columbus, OH 43210 USA.
[3]Department of Geography, The Ohio State University, Columbus, OH 43210 USA.
[4]Institute of Geography, Russian Academy of Sciences, Moscow, Russia.
[5]Department of Geography and Geosciences, University of Louisville, Louisville, KY 40292 USA.

Contents of this file

Text S1
Figures S1 to S6
Tables S1 to S2

Text S1.

Pit and shallow core $\delta^{18}O$ data from the QIC

Most of the pits excavated on the summit dome of the QIC were 2 to 3 meters deep in order to capture the snowfall of the previous thermal year. Of the 24 field seasons conducted on this ice cap from 1974 to 2016, 6 resulted in the collection of samples from pits alone, 6 resulted in the collection of shallow cores alone (or a deep core, in the case of 2003), and 12 resulted in the collection of both pit samples and shallow cores (Fig S1). During the first deep drilling expedition in 1983, a shallow core was drilled at the bottom of a 2.6 meter snow pit. The seasonal variations in the $\delta^{18}O$ data are highly reproducible in the 15 profiles for which duplicate sets of samples (shown in red) were collected from pits or a combination of pits and cores.

Dating of 2015/16 shallow cores from QIC and HS

The shallow cores drilled in 2016 from the QIC summit dome (Fig. S2a) and the HS col (Fig. S2b) were dated using seasonal variations in $\delta^{18}O$ and the concentrations of nitrate (NO_3^-) and insoluble dust. The samples from these cores were cut, bagged, melted and bottled at the field site under less than ideal conditions for recovering the highest quality dust data. Thus, while the $\delta^{18}O$ values would not be altered by such handling, the seasonal aerosol variations may not be as well-defined as they would be had the samples been cut directly from the cores in the BPCRC freezer and prepared for analysis under environmentally controlled laboratory conditions. Nevertheless the dust, and especially the nitrate concentrations (smoothed with 3-sample running means) show wet (dry) season concentrations that are in phase with low (high) $\delta^{18}O$ values in the cores. These seasonally varying constituents allow thermal year determinations in the cores, especially in the QIC core at depths where the high frequency $\delta^{18}O$ variability associated with specific snow events is smoothed over time. The seasonal $\delta^{18}O$ variations in the 2016 QIC summit core are difficult to distinguish, thus other seasonally varying parameters were used to date the core.

Criteria for determination of major ENSO events

Strong El Niño events were selected using the Oceanic Niño Index (ONI) for DJF (http://www.cpc.noaa.gov/products/analysis_monitoring/ensostuff/ensoyears.shtml), as the $\delta^{18}O$ values in the QIC and HS originate in snow deposited mainly in the austral summer. The SSTs, 500mb-Ts, and CTTs used to create Figure 6 (main text) are average DJF values. ONI values < -1.0 and > +1.0 were chosen to determine strong events. As Table S1 shows, 10 years meet those criteria. These are emphasized in Table S1; however, no isotopic data exist from the QIC or HS for the 1997/98, 1998/99, and 2009/10 events as no field programs were conducted on either ice field in 1998, 1999 and 2010.

500 mb during austral summers in the QIC vicinity

Reanalysis DJF 500mb-T data from NOAA NCEP-NCAR CDAS-1 are plotted from DJF 1973/74 to DJF 2016/17 at grid point 15°S, 70°W to illustrate that the mid-tropospheric temperature during the austral summer of the 2015/16 El Niño was the warmest in the period under consideration in this study (Fig. S3).

Stratigraphy and density of the 2016 Quelccaya summit pit

The density, visible stratigraphy, and $\delta^{18}O$ in the 2016 Quelccaya summit pit (Fig. S4) shows that the bottom of the 2015/16 thermal year is marked by a dust layer. Below the lower annual boundary are multiple ice layers in dense firn, which may have served to inhibit downward movement of surface or near surface meltwater.

Retreat of the QIC ice margin

A western margin of the QIC was photographed from the ground in 2000, 2005, 2015, and 2016 (Fig. S5). The glacier edges in the 2000, 2005, and 2016 photographs were superimposed upon the 2015 image (Fig. 5a, main text). In Fig. 5b (main text), the position of the glacier edge was determined manually based on the *in situ* 2000 and 2005 photographs, and the high-resolution visible satellite images for 2015 and 2016. As for the ground images, the glacier edges are superimposed on the 2015 satellite image. These satellites images were acquired by DigitalGlobe's WorldView-3 Satellite on 29 June 2015 and 2 July 2016 and were obtained from TerraServer.com. The area covered by the glacier within the bounds of the satellite image was estimated using the georeferenced glacier boundaries in a Peru96/UTM zone 19S projection (EPSG:5389). All data processing and calculations (Table S2) were performed using the QGIS software.

Tests of significant differences between ENSO-inclusive and exclusive R fields

The difference between the ENSO-inclusive and ENSO-exclusive spatial correlation patterns is determined by converting the respective correlation coefficients into z-scores using Fisher's r to z transformation (equation 1).

$$(1)\quad z = 0.5 * ln\left(\frac{1+r}{1-r}\right)$$

Next the z-observed value is calculated to determine the level of significance for the difference between the spatial correlations (equation 2). Here $n_1 = 24$, the number of observations for the ENSO-inclusive case and $n_2 = 17$, the number of observations for the ENSO-exclusive case and z_1 and z_2 are the corresponding z-scores for the two cases.

$$(2)\quad z_{obs} = \frac{(z_1 - z_2)}{\sqrt{\frac{1}{n_1-3}+\frac{1}{n_2-3}}}$$

For 90% and 95% significance, the critical z_{obs} values are ±1.645 and ±1.960, respectively. Both Quelccaya and Huascarán $\delta^{18}O$ show strong positive correlations with SSTs in the tropical Pacific (Fig. 6a, d, main text); however, the magnitudes of these correlations drop considerably when major ENSO events are removed (Fig. 6g, j, main text). For Quelccaya, the difference in the spatial patterns is significant (Fig. S6a) while for Huascarán, the difference is much less (Fig. S6b). This indicates that the relationship between SSTs and $\delta^{18}O$ from Quelccaya is driven largely by major ENSO events since the relationship is much weaker when these seven events are removed. In the case of Huascarán, ENSO may be influential in the composition of $\delta^{18}O$, but to a much lesser extent than for Quelccaya. This is also the case for 500mb temperatures (Fig. S6c, d) and cloud top temperatures (Fig. S6e, f). The differences in the spatial patterns of the $\delta^{18}O$/500 mb-T and $\delta^{18}O$/CTT for Quelccaya occur mainly in the tropical Pacific and tropical North Atlantic (which is the ultimate moisture source for Quelccaya precipitation), while for Huascarán the significant differences are virtually negligible.

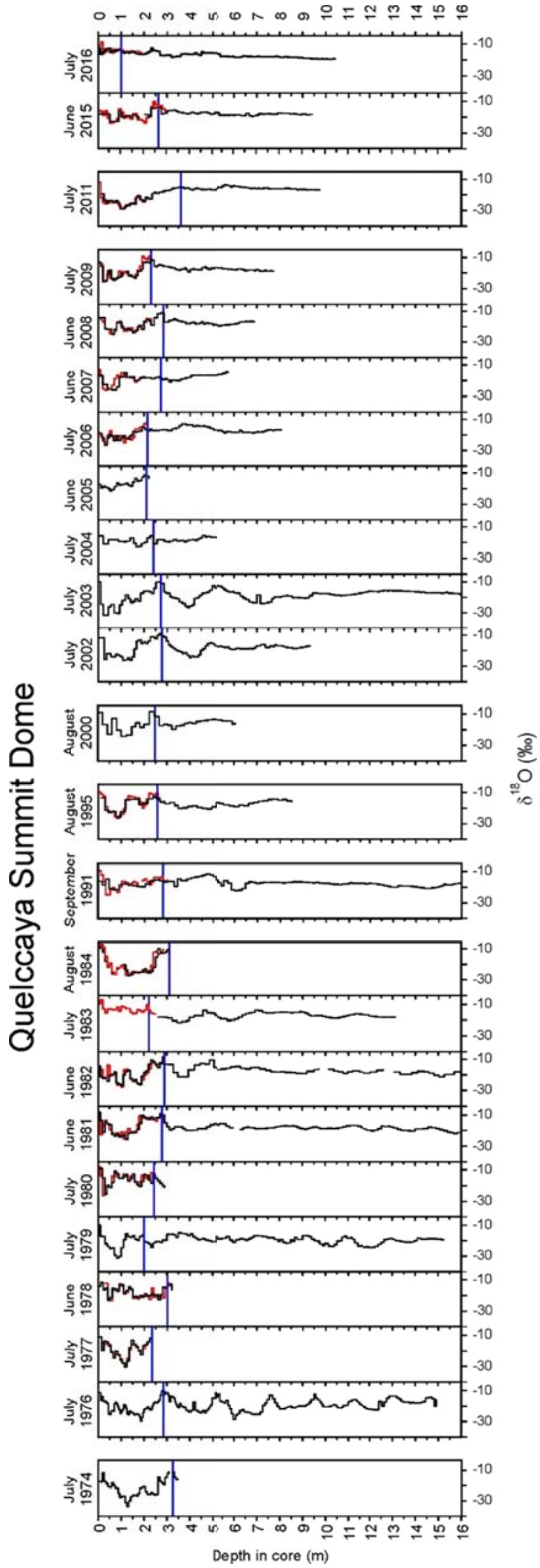

Figure S1. $\delta^{18}O$ data from pit and shallow core samples from the summit dome of the QIC. Above each column is the month and year of the sample collection, which always occurred during the austral winter (dry season). The top thermal year (TY1) is marked in each profile. The range of the x-axis is identical for each profile. Where more than one set of samples was collected during a field season, the additional data are shown in red.

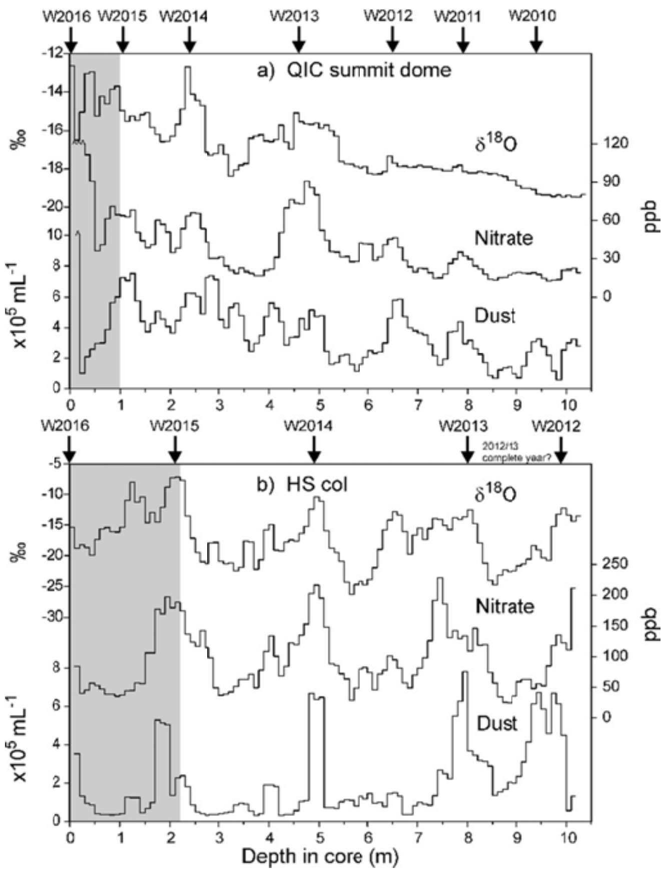

Figure S2. Data from shallow cores drilled in July 2016 from (a) the Quelccaya summit dome and (b) the Huascarán col demonstrate time scale development based on seasonal variations in $\delta^{18}O$ and concentrations of nitrate and insoluble dust with diameters between 0.63 and 20 µm. Austral winters are indicated by the prefix "W". The nitrate and dust concentrations are smoothed with 3-sample running means to minimize noise, while the $\delta^{18}O$ profiles are not smoothed. All the samples in these cores were melted and bottled in the field. The top thermal year layers are shaded.

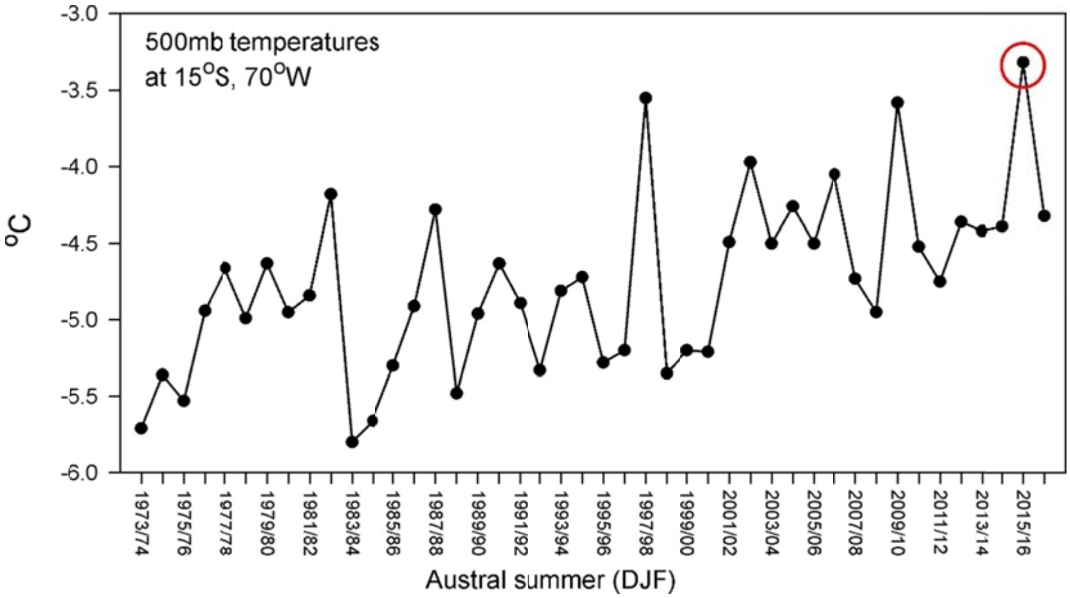

Figure S3. Temperatures at 500 mb in the vicinity of the Quelccaya ice cap from DJF 1973/74 to 2016/17. The 2015/2016 El Niño year is marked by a red open circle. Data are from NOAA NCEP-NCAR CDAS-1 MONTHLY Intrinsic Pressure Level Temperature [*Kalnay et al.*, 1996].

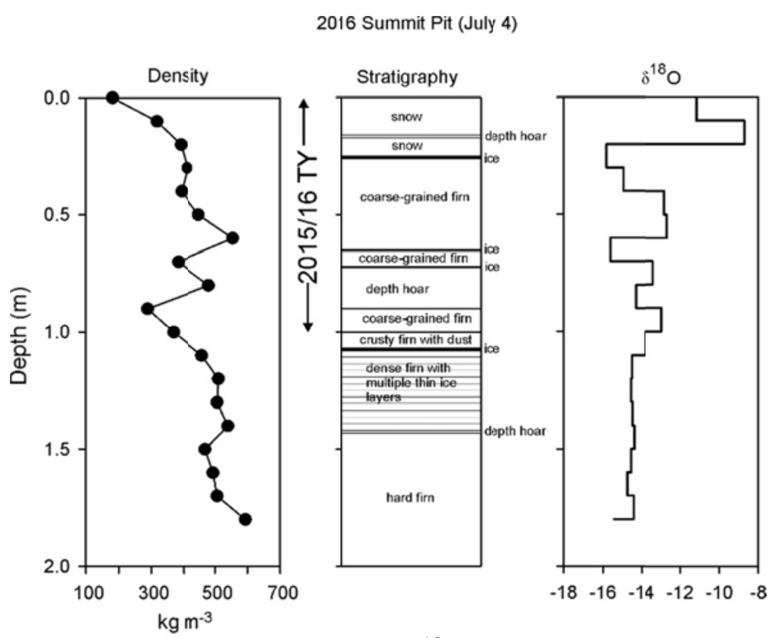

Figure S4. Density, visible stratigraphy, and δ^{18}O of the 2016 QIC summit dome pit. The 2015/16 thermal year is noted.

Figure S5. Individual photos of the Quelccaya ice cap margin from which the ice margin composite in Fig. 5a (main text) and the 2000 and 2005 composite in Fig. 5b (main text) are created.

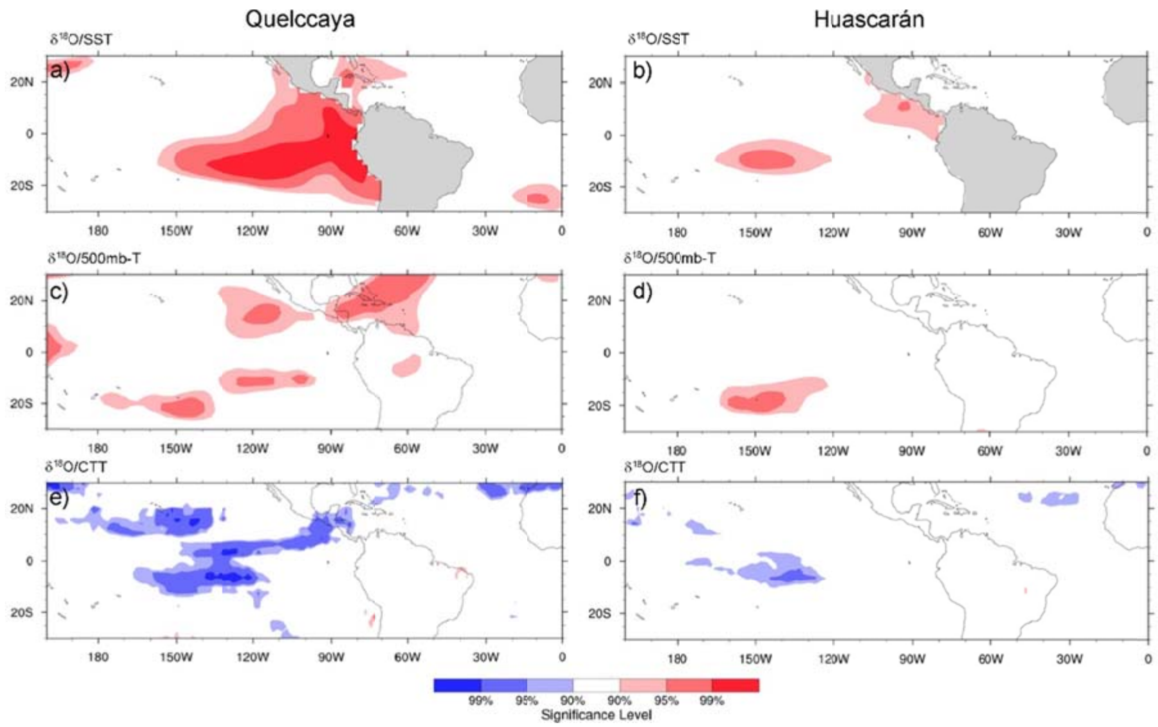

Figure S6. Spatial patterns of the differences between z-scores of the correlation coefficients for ENSO-inclusive and ENSO-exclusive $\delta^{18}O$/SST for (a) QIC and (b) HS; (c, d) same as (a, b), except for 500mb-T; (e, f) same as (a, b) except for CTT.

TY	ONI (DJF)	TY	ONI (DJF)	TY	ONI (DJF)	TY	ONI (DJF)
1973/74	***-1.7***	1984/85	-0.9	1995/96	-0.9	2006/07	0.7
1974/75	-0.5	1985/86	-0.4	1996/97	-0.5	***2007/08***	***-1.4***
1975/76	***-1.5***	***1986/87***	***1.1***	*1997/98*	*2.1*	2008/09	-0.7
1976/77	0.7	1987/88	0.8	*1998/99*	*-1.4*	*2009/10*	*1.3*
1977/78	0.7	***1988/89***	***-1.6***	***1999/00***	***-1.6***	***2010/11***	***-1.3***
1978/79	0.0	1989/90	0.1	2000/01	-0.7	2011/12	-0.7
1979/80	0.6	1990/91	0.4	2001/02	-0.2	2012/13	-0.4
1980/81	-0.2	***1991/92***	***1.6***	2002/03	0.9	2013/14	-0.5
1981/82	0.0	1992/93	0.2	2003/04	0.3	2014/15	0.6
1982/83	***2.1***	1993/94	0.1	2004/05	0.7	***2015/16***	***2.2***
1983/84	-0.5	1994/95	0.9	2005/06	-0.7		

Table S1. Oceanic Niño Indices (ONI) for December to February (DJF) from 1973/74 to 2015/16. Notable ENSO events (-1.0 > ONI > 1.0) are emphasized in bold italics; the strong 1997/98, 1998/99, and 2009/10 events for which no $\delta^{18}O$ data exist are only italicized.

Years	Area (m^2)
2000	230,550
2005	181,518
2015	86,705
2016	74,471

Table S2. Area of ice cover during the dry season for the region along the western margin of the QIC outlined in Figure 5 (main text).